

# Fabrication of Yttria/Niobium Laminar Composites by Plasma Spraying

M. Boncoeur & G. Schnedecker

Commissariat à l'Énergie Atomique, Centre d'Études de Saclay, DTA/CEREM/DTM/SERC,  
91191, Gif-Sur-Yvette Cedex, France

(Received 17 September 1993; revised version received 11 January 1994; accepted 7 February 1994)

## Abstract

The present study shows that it is possible to obtain, by plasma spraying, laminar composites made of alternate thin layers of a ceramic and a metal. One example consists of nine layers of yttria and of niobium, each 0.3 mm thick. The microstructures and the flexural characteristics of these composites have been studied for the as-sprayed product and for the product heat-treated under vacuum at 1400°C for 100 h. It has been shown that the as-sprayed product is brittle, whereas the thermally treated product becomes pseudo-plastic: stresses larger than 150 MPa are still well sustained by test bars 2.7 mm thick bent by 1 mm. This difference in behaviour is a result of the reorganisation of the microstructure of the metal to give it a plasticity close to that of a niobium sheet. A parallel is drawn between the damage observed using a scanning electron microscope in pieces subjected to the bend test and the shape of the stress/deflection curves.

In der vorliegenden Arbeit wird gezeigt, daß es mittels Plasmasprühen möglich ist, laminierte Verbunde aus alternierenden, dünnen Keramik- und Metallschichten herzustellen. Ein Beispiel ist ein Verbund aus 9 Schichten, jede 0.3 mm dick, Yttriumoxid und Niob. Die Gefüge und die Biegecharakteristiken dieser Verbunde wurden direkt nach dem Sprühen und nach einer Wärmebehandlung im Vakuum bei 1400°C für 100 Stunden untersucht. Es konnte gezeigt werden, daß die unbehandelten Proben spröde sind, während sich die wärmebehandelten pseudoelastisch verhalten: 2.7 mm dicke Stangen, die 1 mm gebogen wurden, konnten Spannungen größer als 150 MPa standhalten. Dieses unterschiedliche Verhalten resultiert aus der Reorganisation des Metallgefüges; die Plastizität ist ähnlich der einer Niobplatte. Es wird ein Vergleich zwischen der Schädigung an Biegeproben,

beobachtet mit dem Rasterelektronenmikroskop, und der Form der Spannungs/Durchbiegekurven angestellt.

Cette étude montre qu'il est possible d'obtenir par projection plasma des composites lamellaires constitués de couches fines alternées de céramique et de métal. Un exemple est celui d'un composite à 9 couches, chacune de 0.3 mm d'épaisseur d'oxyde d'yttrium et de niobium. Les microstructures et les caractéristiques en flexion ont été étudiées d'une part sur le composite brut de projection et sur le composite après traitement thermique sous vide à 1400°C pendant 100 h. On a montré que le produit brut de projection est fragile et devient pseudo plastique après traitement thermique: des contraintes supérieures à 150 MPa sont encore bien supportées par des barrettes test de 2.7 mm d'épaisseur avec une déformation de 1 mm. Cette différence de comportement est le résultat d'une réorganisation de la microstructure du métal lui conférant une plasticité proche de celle d'une feuille de niobium. On fait un parallèle entre les dommages observés par microscope électronique à balayage sur les pièces après test de flexion, et la forme des courbes contrainte/déformation.

## 1 Introduction

Recent publications have shown that laminar composites consisting of thin alternate layers of ceramic and metal have advantageous mechanical properties.<sup>1–3</sup> More specifically, the sudden fracture of fragile ceramics would be replaced by a much more gradual non-fragile fracture. One of the simple and industrial methods of manufacturing laminar composites is plasma spraying. The purpose of the study is to verify the feasibility of manufacturing a niobium/yttria laminar composite

using this method, and then to verify its mechanical strength when bent.

These two materials have been chosen both for their good mechanical compatibility at high temperature and for the low difference between their thermal expansion coefficients at 1000°C which are  $8 \times 10^{-6}/^{\circ}\text{C}$  and  $9 \times 10^{-6}/^{\circ}\text{C}$  for niobium and for yttria, respectively. The as-sprayed products consist of micro-droplets splattered on top of each other and not very strongly bonded. Hence, even the metal deposits are brittle. The effect of a heat treatment at 1400°C on regenerating the plasticity of the metal and on the overall mechanical strength of the  $\text{Y}_2\text{O}_3/\text{Nb}$  laminar composite was assessed.

## 2 Experimental Methods

### 2.1 Elaboration of the laminar $\text{Y}_2\text{O}_3/\text{Nb}$ composite

$\text{Y}_2\text{O}_3$  and Nb powders from H. C. Starck were sprayed with a Plasmatechnik gun under an argon atmosphere, in a CEA-type patented facility. The relative motions gun/sample are automated. The layers, each 0.3 mm thick, are sprayed successively one over the other without interruption of the gun. The powder distributor is simply rocked from one container filled with the oxide to the other filled with the niobium. Plates of  $105 \times 90$  mm are fabricated. The quality of the multilayer composite, in particular the uniformity of the layer thickness and the absence of defects at the interfaces is well under control. The reference composite is made of nine layers 0.3 mm thick (to about 0.05 mm accuracy); five are made of  $\text{Y}_2\text{O}_3$ , and the two external ones and the other four alternate internal ones are made of niobium.

The macrographic aspect of the as-sprayed nine-

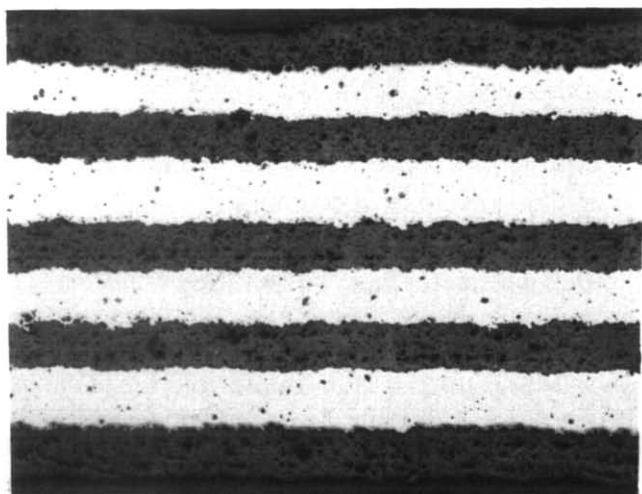
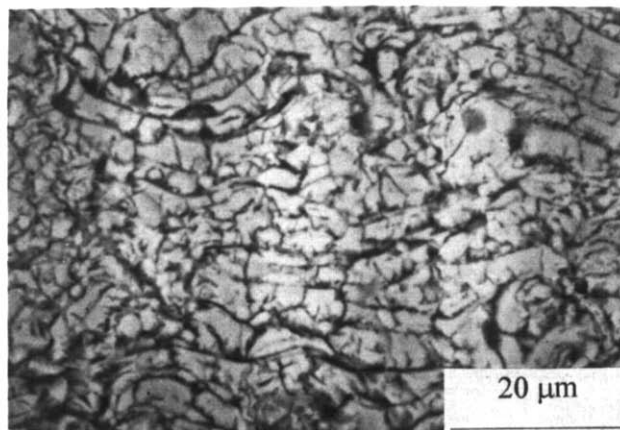
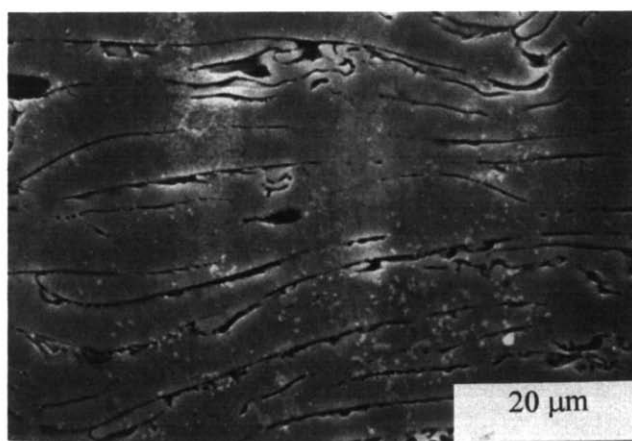


Fig. 1. Macrostructure of as-sprayed  $\text{Y}_2\text{O}_3/\text{Nb}$  laminar composite. Magnification  $\times 32$ ; dark layers,  $\text{Y}_2\text{O}_3$ ; light layers, Nb.



(a)



(b)

Fig. 2. Macrostructure of (a)  $\text{Y}_2\text{O}_3$  and (b) Nb layers in as-sprayed laminar composite.

layer composite is shown in Fig. 1. The porous structure of  $\text{Y}_2\text{O}_3$  and Nb can be seen. The bonding at the interface is good. The uniformity of the layer thickness is already satisfactory. The volume fraction of niobium is close to 44.4%. One can see in Fig. 2 that the as-sprayed  $\text{Y}_2\text{O}_3$  layers are stratified and

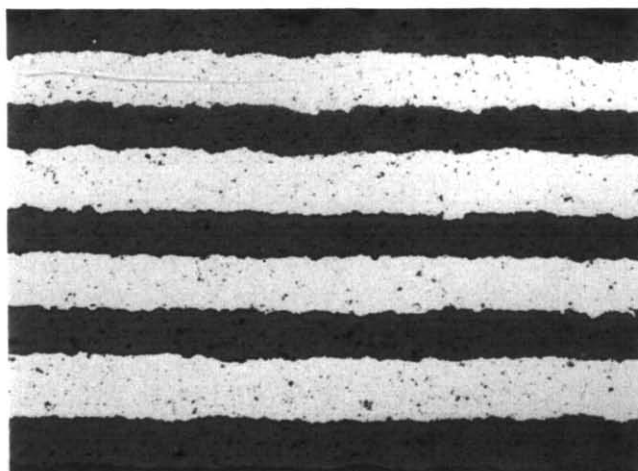


Fig. 3. Macrostructure of heat-treated  $\text{Y}_2\text{O}_3/\text{Nb}$  laminar composite. Magnification  $\times 32$ ; dark layers,  $\text{Y}_2\text{O}_3$ ; light layers, Nb.

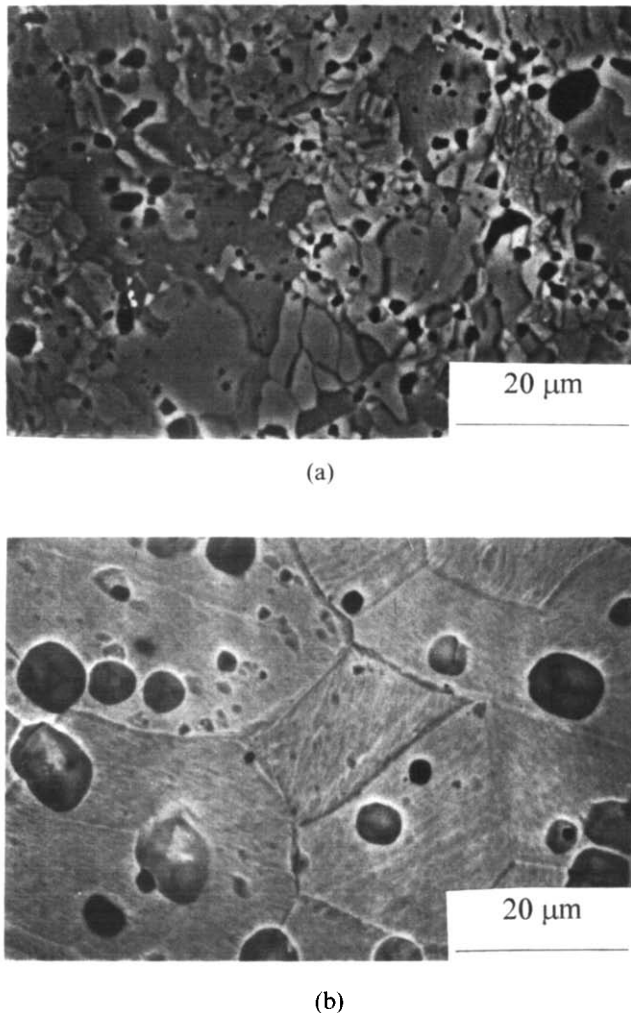


Fig. 4. Microstructure of (a)  $Y_2O_3$  and (b) Nb layers in heat-treated laminar composites.

microcracked. The porosity is made of microcracks and of more compact pores with an equivalent mean diameter which can reach about  $10\ \mu\text{m}$ . The microstructure of the Nb layers in the as-sprayed composite is shown in the same figure. One distinguishes the stratification of the metal due to the stacking of droplets at impact. A fine porosity decorates in some places the limits of the lamellae, larger pores of about  $10\ \mu\text{m}$  are uniformly distributed.

Heat treatment to rearrange the microstructure of the yttrium oxide and the niobium is carried out at  $1400^\circ\text{C}$  for 100 h. Previous studies have shown the onset of sintering for the yttrium oxide under these conditions<sup>4</sup> and a very advanced state of the sintering of niobium (Boncoeur, M. & Schneidecker, G., unpublished). It can be seen in Fig. 3 that the macrostructure of the multilayer and the quality of the bonding at the interface do not change in a visible manner during this heat treatment. The microstructure of the yttrium oxide heated at  $1400^\circ\text{C}$  is modified. It can be seen in Fig. 4 that the lamellae have disappeared. One distinguishes zones under reorganisation with very little polygonal grains of about 1 micron and elon-

gated grains longer than  $10\ \mu\text{m}$ . The porosity is becoming spheroidal and is located preferentially at the grain boundaries. The microstructure of the Nb shown in the same figure is also highly modified. Polygonal grains of less than  $30\ \mu\text{m}$  have appeared. The porosity, here enhanced by chemical attack of the sample, is becoming more spheroidal and is distributed in the grains and to a lesser degree at the boundaries.

## 2.2 Three-point flexural tests; microscopic examination of the tested samples

For this first study, non-standard flexural test bars have been used. They are parallelepipeds of 25 mm length and of 4 mm width. Their thickness is that of the elaborated plates, i.e. 2.7 mm. The support surfaces are as-sprayed and the lateral ones were cut with a diamond saw. In order to get significant values, a minimum of six results were used for each of the materials. The  $Y_2O_3$  and Nb layers are parallel to the support surfaces in all of the test bars. Stainless steel rollers of 4 mm diameter are used with a spacing of 20 mm. The stainless steel loading knife has a support radius of 1.5 mm. The speed of the cross bar of the Instron machine is 0.2 mm/min.

Microscopic examinations of the bent bars have been made in order to evaluate their degradation process and in some cases their rupture process. A parallel between the post-test observations and the form of the stress/deflection curves was drawn.

## 3 Results

### 3.1 Three-point flexural tests

The stress/deflection curve of an as-sprayed composite test bar is reproduced in Fig. 5. After a slight slipping of the test bar on its supports, a linear increase of the curve is observed. The maximal rupture stress is 174 MPa. A first step decrease of the stress is visible, followed by an increase with a lower slope up to a peak of 123 MPa. Several steep stress drops appear at higher deflection with, in between, stress increases with lower and lower elasticity modulus. After a deflection of the order of 0.3 mm the test bar is broken.

The curve obtained with a heat-treated test bar is plotted in Fig. 6. The first part of the curve is linear up to a stress of about 170 MPa. In the second part of the curve, the slope decreases regularly with the deflection up to a maximal stress of 259 MPa obtained for a displacement of 0.7 mm. The third part is a steep stress decrease down to 170 MPa. For the fourth part, the load increases in a non-linear fashion and then reaches a quasi-plateau of deformation at constant stress of about

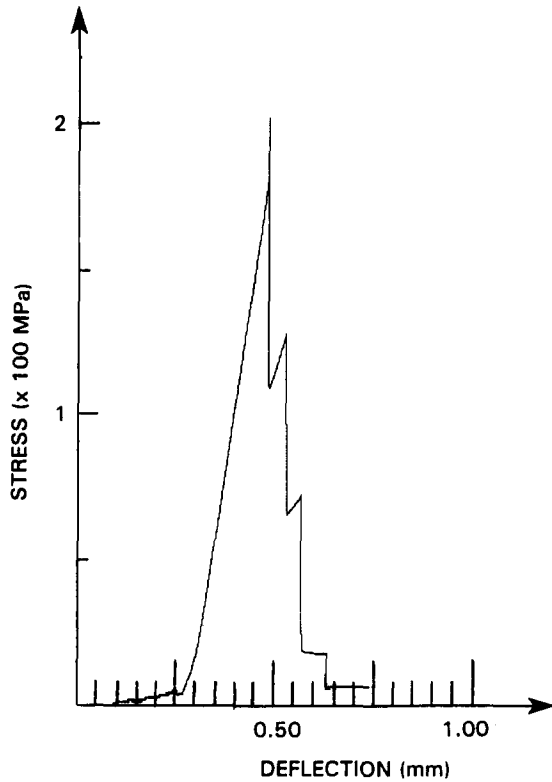


Fig. 5. Stress-deflection curve of as-sprayed laminar composite in three-point bending test.

194 MPa. The flexural test is stopped at this stage without rupture of the test bar. It can therefore be seen that the main effect of heat treatment is to eliminate brittle rupture of the composite.

### 3.2 Post-test micrographic examination of the test bars

The macrograph in Fig. 7 enables the observation of the zone damaged by the rupture of an as-sprayed composite test bar. The global aspect is that of a brittle rupture in steps of irregular width.

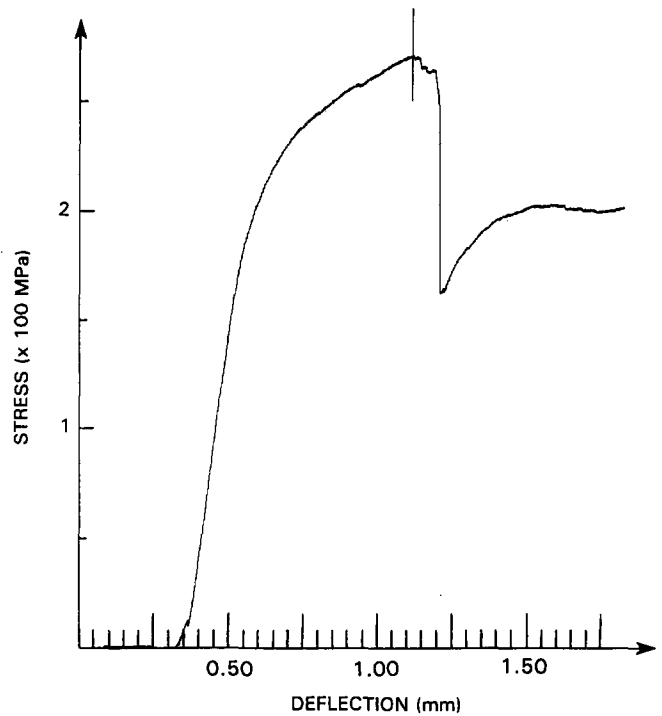


Fig. 6. Stress-deflection curve of heat-treated laminar composite (1400°C, 100 h) in three-point bending test.

A main crack has developed on the lower face subjected to the maximal tensile stress, in  $Y_2O_3$  having a very low tensile strength of the order of 10 to 20 MPa (Boncoeur, M. & Schnedecker, G., unpublished). The crack starts close to the vertical load plane of the test bar. It does not propagate straight but is deflected along the Nb layers. One observes, particularly in Fig. 7, two secondary interfacial shear cracks which propagate on the lower surfaces of the second and third layer of Nb.

The macrograph of a test bar heat-treated at

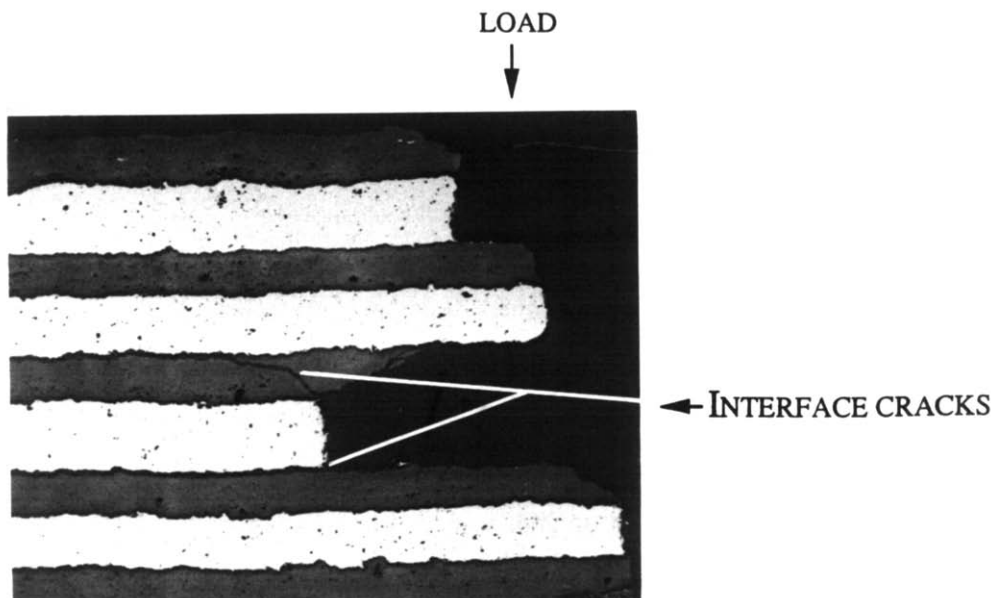


Fig. 7. Fracture zone of as-sprayed laminar composite in three-point bending test. Magnification  $\times 32$ .

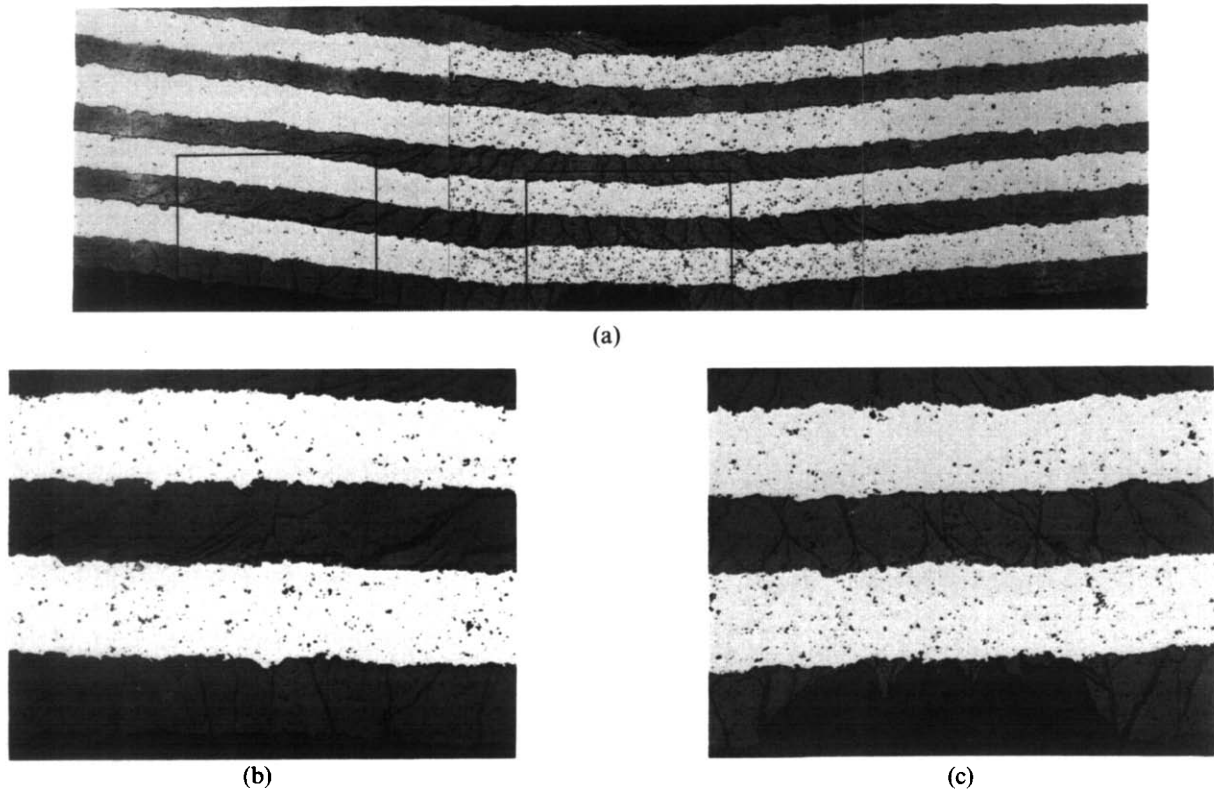


Fig. 8. Macrographs of heat-treated laminar composite (1400°C, 100 h) in three-point bending test. (a) Magnification  $\times 28$ ; (b) and (c) magnification  $\times 64$  of (b) left-hand and (c) right-hand boxes in (a).

1400°C and bent is presented in Fig. 8(a). The test bar is not broken. It is subjected to a principal flexural effect around the loading knife and in addition to a slight bending in the opposite direction around the two supporting rollers. The damage is caused by a network of microcracks, in the  $Y_2O_3$  layers, in the area of maximum strain, i.e. approximately 4–5 mm either side of the plane at which the load is applied. Beyond this, a few rare microcracks can be detected in the two lowest

$Y_2O_3$  layers up to the two support areas on the bend.

One can see in Fig. 8(c) that the Nb layers are curved and free of cracks. All the  $Y_2O_3$  layers are crossed by microcracks pointing towards the

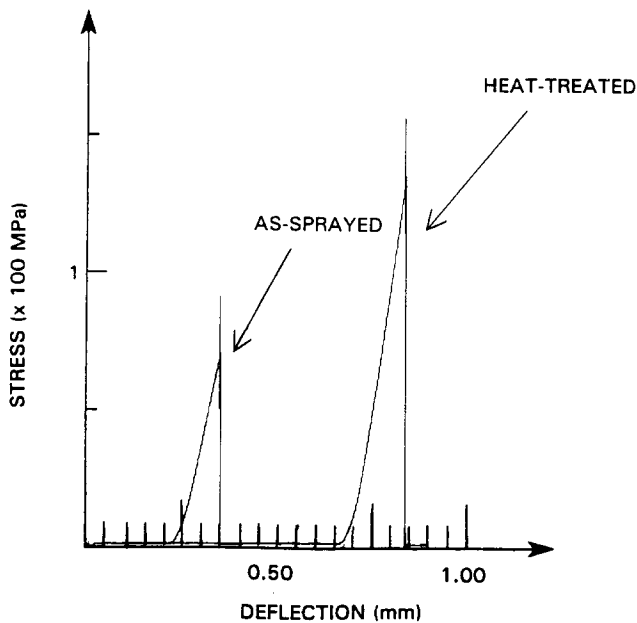


Fig. 9. Stress-deflection curves of as-sprayed and heat-treated  $Y_2O_3$  samples in three-point bending test.

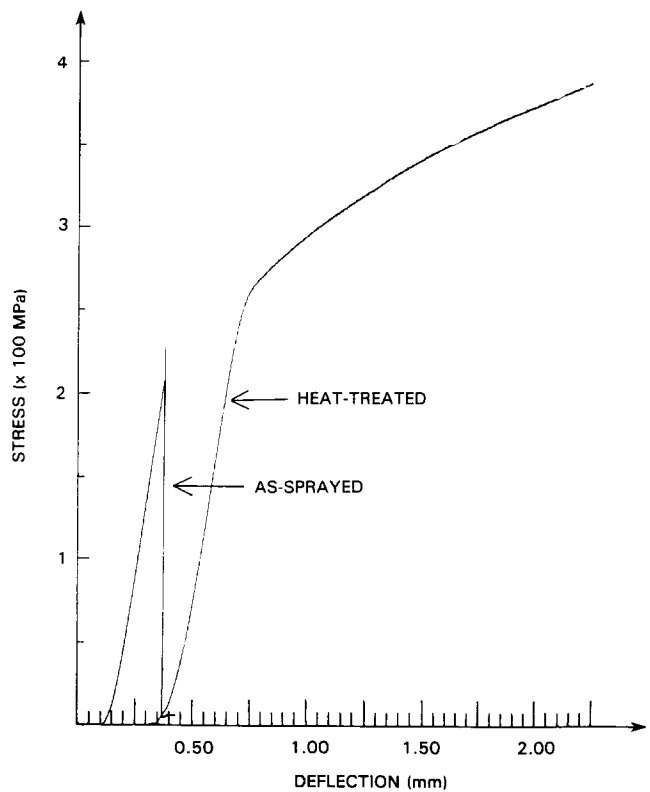


Fig. 10. Stress-deflection curves of as-sprayed and heat-treated Nb samples in three-point bending test.

bending centre of the loading knife. Their density is higher in the lower layers. The lowest  $Y_2O_3$  layer is debonded over a 2–3 mm width. Under the effect of the tensile stresses the cracks have been initiated vertically, then have split in multiple oblique microcracks which never penetrate into the Nb. The upper  $Y_2O_3$  layer, under the effect of the knife, is also slightly delaminated; the cracks are not numerous but close and parallel to the loading surface of the knife. The volume of material involved by the microcracks network is a well-limited sector of a quasi-cylindrical ring. Fig. 8(b) shows, beyond the ring sector, very open interfacial shear cracks on the upper surfaces of the three lower Nb layers.

## 4 Discussion

### 4.1 Behaviour of $Y_2O_3$ and Nb alone, in sprayed layers.

The rupture of as-sprayed and heat-treated  $Y_2O_3$  is always brittle, as can be verified in Fig. 9. The maximal rupture stress increases from 66 MPa to 120 MPa with the heat treatment, due to the microstructural reorganisation of the oxide and the porosity reduction. For the as-sprayed Nb the failure is also always brittle, as can be seen in Fig. 10. This brittleness is due to the microstructure of the sprayed metal, made of stacked lamellae separated one from the other by vacuoles of planar shapes. The mean rupture strength is 200 MPa for 0.45 mm deflection. The niobium annealed at 1400°C for 100 h recovers its plasticity. The mean elastic limit is 184 MPa. For a deflection of 2.2 mm no test bar is broken and the mean stress is 315 MPa. Under the same heat treatment and flexural test conditions the mean stress for a niobium sheet is 325 MPa.

The micrographic examination shows that the heat treatment enabled a reorganisation of the metal microstructure. The lamellar stacking slightly bonded structure with a brittle behaviour, shown in Fig. 2, changes to an equiaxial grain microstructure with a plastic deformation, as shown in Fig. 4. The porosity of the metal has also decreased from 11% to 7.5%, the pore becoming more spherical in shape.

### 4.2 Correlation of flexural curves and microstructural observations

It must be noted that the as-sprayed composite consists of brittle layers of  $Y_2O_3$  and Nb which are strongly bonded together. In accordance with the models described earlier, especially those by Warren<sup>5</sup> and Mecholsky<sup>6</sup> for long fibre-reinforced composites, the fracture should be brittle under

these conditions. This is indeed what was observed. In the heat-treated material, the Nb becomes plastic, the oxide remains brittle and the bonding between them remains of good quality. It obviously performs differently to the as-sprayed material. Using published results for laminar composites<sup>1–3</sup> or for long fibre-reinforced composites,<sup>5</sup> an attempt can be made to draw a correlation between the damage observed using the scanning electron microscope and the shape of the flexural curves plotted in Figs 5 and 6.

For the as-sprayed composite or heat-treated at 1400°C, the first part of the curves corresponds to an initial elastic loading of the material without damage. The linear portion stops when the critical stress of formation of the first crack is reached in the weakest material at the most stressed point: here in the first lower layer of  $Y_2O_3$ . In the as-sprayed composite the first crack abruptly crosses the first layer of  $Y_2O_3$  and the first layer of brittle Nb, inducing a large drop of the load in Fig. 5. The following increase in stress corresponds to the energy consumed to propagate the first secondary shear crack at the first  $Y_2O_3$ /Nb interface concerned. When the deformation is large enough a new couple of  $Y_2O_3$  and of Nb layers are broken and the stress drops abruptly. A new interfacial shear crack starts and propagates at the second  $Y_2O_3$ /Nb interface, inducing the second small stress increase on the stress/deflection curve. This cycle repeats until the total rupture in irregular steps of the test bar.

For the composite heat-treated at 1400°C, the second part of the curve in Fig. 6, above the critical stress for the start of the first crack in  $Y_2O_3$ , corresponds to the set up of the microcracks network in  $Y_2O_3$  with a decrease of the stiffness of the laminar composite. This loss of stiffness is regular as long as the microcrack network develops homogeneously. The maximum density of micro-cracks is reached in  $Y_2O_3$  when the composite withstands the maximum load. The Nb layers are plastically elongated and stop the propagation of the micro-cracks. The drop of the stress in the third part of the curve probably corresponds to a sudden opening of the  $Y_2O_3$  cracks which withstand the largest tensile and shear stresses. In each of the oxide layers, one of the open cracks induces the formation of an interfacial shear crack at the surface of the plastic Nb layer which supports it. The propagation of those shear cracks consumes energy and explains the first observed stress increase which constitutes the fourth part of the curve. One can expect that a succession of similar mechanisms will occur for larger deflections of the test bar.

Chen & Mecholsky<sup>1</sup>, for example, have already shown that an alumina/nickel laminar composite

obtained by tape casting, fractured in a much more gradual manner under flexural stress than monolithic alumina. It is certain that the present heat-treated  $Y_2O_3/Nb$  laminar composite shows a behaviour which is even closer to that of a plastic metal.

## 5 Conclusion

It is possible to elaborate by plasma spraying a laminar composite made by alternate stacking of ceramic and metal layers: yttria and niobium for example. One can observe that after a heat treatment which restores plasticity to the metal, the composite shows an appreciable pseudo-plasticity in a three-point flexural test. These laminar composites have very attractive characteristics for the realisation of extended composite areas a few millimeters thick. Work is in progress in order to specify their behaviour and to better evaluate

their mechanical, physical and chemical advantages compared to monolithic ceramics.

## References

1. Chen, Z. & Mecholsky, Jr, J. J., Toughening by metallic lamina in nickel/alumina composites. *J. Am. Ceram. Soc.*, **76**(5) (1993) 1258-64.
2. Chou, T. C., Nieh, T. G., Tsui, T. Y., Pharr, G. M. & Oliver, W. C., Mechanical properties and microstructures of metal/ceramic microlaminates: Part 1. Nb/MoSi<sub>2</sub> systems. *J. Mat. Res.*, **7**(10) (1992) 2765-73.
3. Chou, T. C., Nieh, T. G., McAdams, S. D., Pharr, G. M. & Oliver, W. C., Mechanical properties and microstructures of metal/ceramic microlaminates: Part II. Mo/Al<sub>2</sub>O<sub>3</sub> system. *J. Mat. Res.*, **7**, (1992) 2774-84.
4. Gasgnier, G., Baumard, J. F., Boncoeur, M. & Bourgoin, M. The effect of titania addition on the sintering of yttria. In *Euro-Ceramics II*, Vol 1. Ed. G. Ziegler & H. Hausner pp. 499-503.
5. Warren, R. (ed.), *Ceramic-Matrix Composites*. Blackie, Glasgow and London, chapter 4.
6. Mecholsky, J. J. Evaluation for mechanical property testing methods for ceramic matrix composites. *Ceram. Bull.*, **65**(2) (1986) 315, 324.